Available online at www.sciencedirect.com
ScienceDirect
Journal of Power Sources 158 (2006) 825–830
JOURNAL OF POWER SOURCES
www.elsevier.com/locate/jpowsour

On the reaction in the lead–acid battery (as the special review-article by the 2005' Gaston Planté Medal recipient)

Zen-ichiro Takehara

Kyoto University (Professor emeritus) 6-9-1, Goryo-oheyama-cho, Nishikyo-ku, Kyoto 610-1102, Japan

Available online 23 June 2006

It is my great pleasure to be awarded with the 2005' Gaston Planté Medal for significant contribution to the development of lead–acid battery science and technology. I would like to thank most heartily to Prof. D. Pavlov of Chairman, and all members of the Organic Committee of LABAT'2005 for the best treatment to select me as a 2005' Gaston Planté Medallist.

The first practical rechargeable lead–acid battery was demonstrated by G. Planté in 1860. The cell was consisted of the rolled two large lead sheets separated by a sheet of felt dipped in sulfuric acid solution, and it was formed by the repeats of charge and discharge in long time. The battery was formed from nine of such cells. Though the nickel–cadmium battery by W. Jüngner in 1899, and recently the nickel–hydrogen battery in 1990, and then the lithium ion battery in 1991 were demonstrated and produced practically, the lead–acid battery has been produced and used as the main battery up to now over about 150 years. The lead–acid battery is the battery for the wide range of applications, e.g., for the starting automobiles, the electric utility load-leveling, and the electric vehicle propulsion, because they have high performance, as which the energy density of 40 Wh kg^{-1}, 80 Wh l^{-1}, the power density of 300 W kg^{-1}, and the cycle life of more than 2000 times.

I wondered why the lead–acid battery has such high performance and it has been produced and used as the main battery over about 150 years and I had the interest for such performances. Thus, I tried to clear the reaction mechanisms of the positive and the negative active materials in lead–acid battery. It is very important to know the reaction mechanism in the lead–acid battery for the improvement of the lead–acid battery and for the development of the new batteries with high performances, such as the lithium ion battery.

I would like to introduce a lecture on some researches by my group at Kyoto University on the reaction of the positive and the negative active materials in the lead–acid battery [1,2].

1. Cathodic reduction of β-PbO_2 to $PbSO_4$ in sulfuric acid solution (discharge reaction of the positive active material) [3–5]

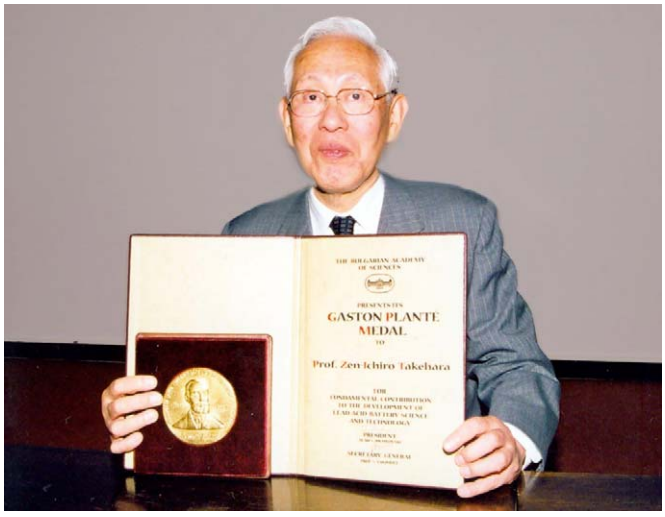

The overall discharge reaction of the lead–acid battery is given by

$$\beta\text{-}PbO_2 + Pb + 2H_2SO_4 \rightarrow 2PbSO_4 + 2H_2O \quad (1)$$

$PbSO_4$ is formed on the positive and the negative electrodes resulting from the discharge of β-PbO_2 and Pb in sulfuric acid solution. These reactions proceed via dissolution–precipitation reactions, that is the formation of Pb^{2+} ions by an electron-transfer step, followed by the precipitation of $PbSO_4$. For the positive electrode, the reaction proceeds as follows:

$$\beta\text{-}PbO_2 + 4H^+ + 2e^- \rightarrow Pb^{2+} + 2H_2O \quad (2)$$

$$Pb^{2+} + HSO_4^- \rightarrow PbSO_4 + H^+ \quad (3)$$

The reaction on the cathodic reduction of β-PbO_2 to $PbSO_4$ was investigated by using a rotating ring-disk electrode. A cyclic voltammogram on the β-PbO_2 disk in 0.5 M H_2SO_4 and a ring current on the Pb, which is kept at the potential of Pb deposition from Pb^{2+} ions, corresponding to the reaction of the disk were measured, as shown in Fig. 1. A peak in the cathodic disk

0378-7753/$ – see front matter
doi:10.1016/j.jpowsour.2005.11.014

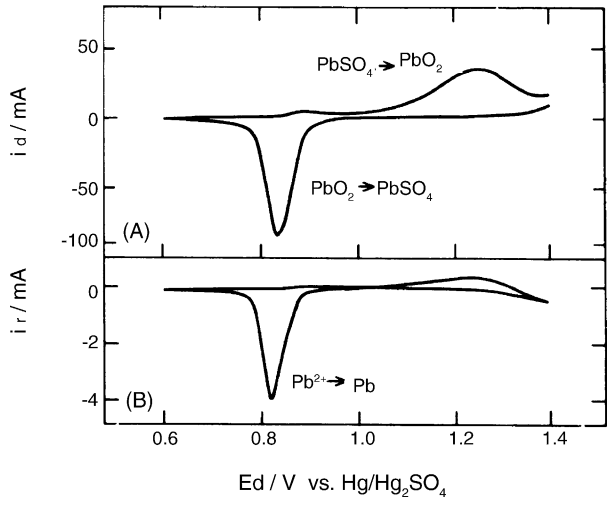

Fig. 1. Cyclic voltammogram on β-PbO_2 disk scanned between 0.6 and 1.4 V vs. Hg/Hg_2SO_4 at scan rate of 10 mV s^{-1} and rotation speed of 33.3 rev s^{-1} (A), and the ring current on Pb ring corresponding to the reaction of the disk (B).

current is due to the formation of $PbSO_4$ during the discharge of β-PbO_2 and a broad peak in the anodic current is due to the formation of β-PbO_2 during the charge of $PbSO_4$. This shows that the discharge and the charge reactions are irreversible and the reaction rate of the discharge is larger than that of the charge. A peak of ring current corresponding to a cathodic current on the disk is observed during the discharge, but the change of cathodic ring current corresponding to a anodic current on the disk is not observed during the charge.

From the changes in the disk current (i_d) and the ring current (i_r) at the potentiostatic discharge, the values of i_r/i_d corresponds to the ratio of the formation rate of Pb^{2+} ions to the precipitation rate are determined, as shown in Fig. 2. The values of i_r/i_d increase after the formation of $PbSO_4$ nuclei, and then decrease until the value reaches 0.03 due to the increase of the precipitation rate. This value, which is smaller than the theoretical value of 0.145, shows that the precipitation rate is much larger than that the formation rate.

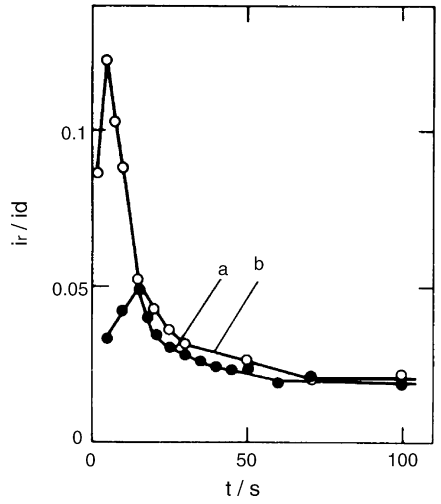

Fig. 2. Changes of i_r/i_d during potentiostatical discharge at: (a) 0.85 V; (b) 0.80 V.

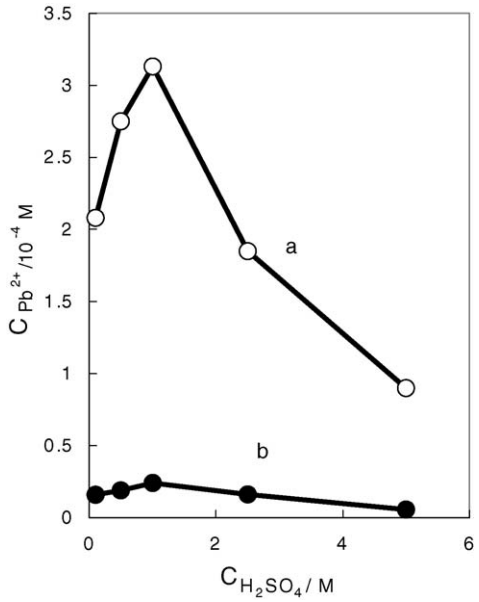

Fig. 3. Concentrations of Pb^{2+} ions: (a) during discharge at 2.5 mA cm^{-2}; (b) calculated from solubility of $PbSO_4$ in different concentrations of the sulfuric acid solution.

The concentrations of Pb^{2+} ions on the electrode surface in different concentrations of sulfuric acid, calculated from the ring current in the steady state at 2.5 mA cm^{-2} discharge are much higher than the equilibrium solubility of $PbSO_4$, as shown in Fig. 3. This shows that not all of the Pb^{2+} ions generated during discharge diffuse out into the sulfuric acid solution, but those dissolved more than the equilibrium concentration, and the colloidal $PbSO_4$ with larger solubility in sulfuric acid solution was formed in the steady state of discharge. Such supersaturation of Pb^{2+} ions can be understood only in terms of the dissolution–precipitation mechanism. Also, at the anodic oxidation of Pb to $PbSO_4$, the same colloidal $PbSO_4$ was formed. But, the concentrations of Pb^{2+} ions in the steady state were smaller than those at the cathodic reduction of β-PbO_2 to $PbSO_4$.

The particle shapes of $PbSO_4$ crystal formed during galvanostatic discharge were observed by SEM. The largest crystal size is obtained in 0.5–1 M H_2SO_4 with the largest Pb^{2+} ion concentration on the surface. The number of $PbSO_4$ nuclei generated on the electrode surface in 0.5–1 M H_2SO_4 may be less those in other electrolyte. Thus the crystal size of $PbSO_4$ increases with discharge current. If the discharge capacity is limited by the passivation of the electrode surface with $PbSO_4$ crystals, the condition forming the large $PbSO_4$ crystals may be favored.

2. Anodic oxidation of $PbSO_4$ to β-PbO_2 in sulfuric acid solution (charge reaction of the positive active material) [6–8]

It is difficult to oxidize the $PbSO_4$ to β-PbO_2 quantitatively, because a large ionic crystal with neither electronic nor ionic conductivity would not be able to oxidize in the same way as soluble species. The dissolving Pb^{2+} ions from $PbSO_4$ crystals of low solubility are oxidized to Pb^{4+} ions on β-PbO_2 with

electronic conductivity and react with H_2O to precipitate on the electrode surface as β-PbO_2, by the following reaction:

$$PbSO_4 \rightarrow Pb^{2+} + {SO_4}^{2-} \quad (4)$$

$$Pb^{2+} + 2H_2O \rightarrow \beta\text{-}PbO_2 + 4H^+ + 2e^- \quad (5)$$

The reaction site is considered to be the interface between $PbSO_4$ and β-PbO_2. To know the place where the reaction proceeds, the $PbSO_4$ electrode was made by the cathodic reduction of β-PbO_2 electrodeposited onto a gold planar plate, in order to avoid the complication caused from the composition of the anodic film on Pb alloy as the grid. This electrode was oxidized at +200 mV versus $PbO_2/PbSO_4$ in 0.5 M H_2SO_4 to 20, 50 and 100% of the electricity passed during the discharge. The surface, the cross-section, and the interface between a gold substrate and the $PbSO_4$ film for each state were observed by SEM, as shown in Fig. 4. The electrode surface oxidized to 20% is perfectly covered with very large $PbSO_4$ crystals. At 50%, β-PbO_2 crystals appear on the electrode surface. At 100%, all parts of the electrode surface is covered with β-PbO_2 crystals. The β-PbO_2 layer is observed in the cross-section of the electrode oxidized to 20% and $PbSO_4$ exists on the β-PbO_2 layer. At 50%, $PbSO_4$ near the electrode surface is oxidized to β-PbO_2. The $PbSO_4$ is observed at 20% but it is not observed beyond 50%, on the interface between a gold plate and the $PbSO_4$ film. Thus, the oxidation of $PbSO_4$ takes place in the deepest part and β-PbO_2 forms at the interface between a gold plate and the $PbSO_4$ layer. Then, the oxidation proceeds at the interior of the film where the two-dimensional change of reaction interface area and the thick β-PbO_2 layer grows. Lastly, $PbSO_4$ remaining near the interface between the electrolyte and the electrode is oxidized without an increase of the reaction interface area.

The potentiodynamic current–voltage curves for the oxidation of $PbSO_4$, which are obtained after the subtraction of the oxygen evolution current from the whole anodic current, are similar to those for a surface reaction controlled electrode reaction. The charge-transfer process of Eq. (5) is very slow. Thus, the anodic reaction rate is considered to depend on both the

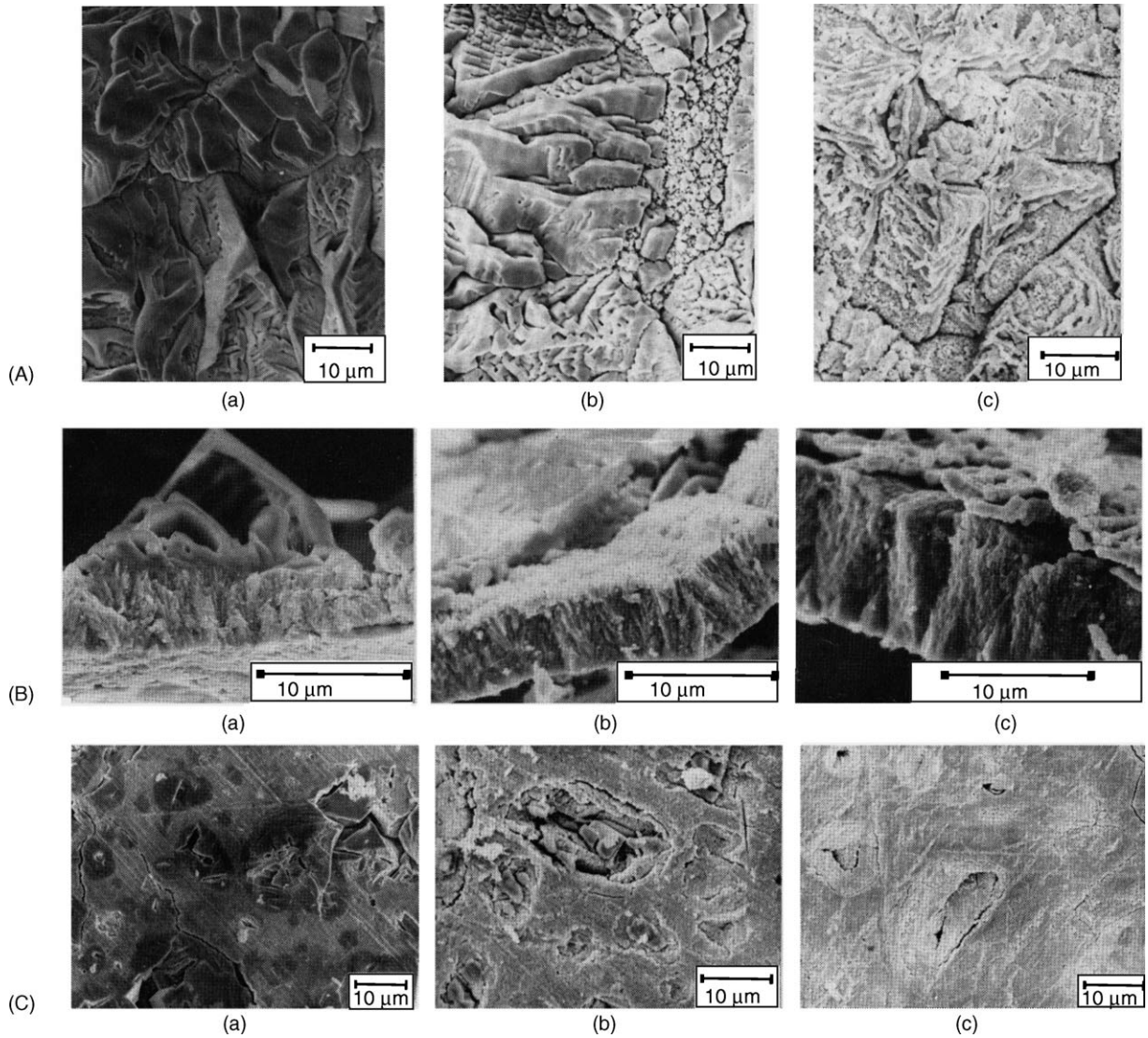

Fig. 4. The electrode surface (A), the cross-section of the electrode (B), and the interface between a gold substrate and the $PbSO_4$ film (C), oxidized at 1.11 V to (a) 20%, (b) 50%, and (c) 100% of the discharge capacity, observed by SEM.

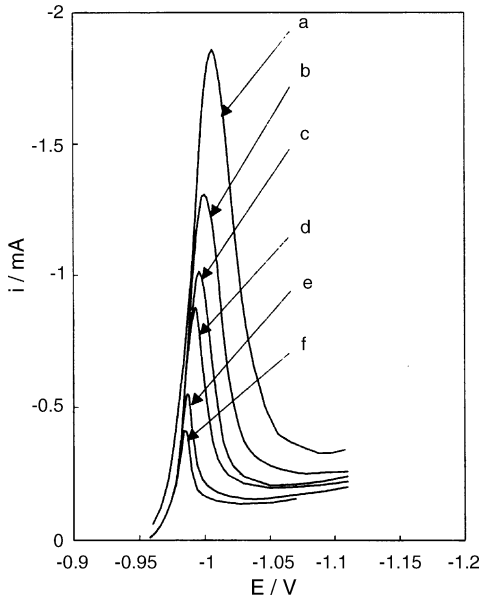

Fig. 5. Current–potential curves of the cathodic reduction of $PbSO_4$ to Pb, on the $Pb/PbSO_4$ electrode prepared by the galvanostatic discharge at 1 mA cm^{-2} for 2 min in 1 M H_2SO_4 by the potential sweet method at various sweep rates: (a) 20 mV s^{-1}; (b) 10 mV s^{-1}; (c) 7 mV s^{-1}; (d) 5 mV s^{-1}; (e) 2 mV s^{-1}; (f) 1 mV s^{-1}.

reaction interface area and the charge-transfer rate at the reaction site. The rate of the reaction of Eq. (5) is increased by the increase of Pb^{2+} ions and the decrease of H^+ ions. Thus, the charge-transfer rate in 0.5 M H_2SO_4 is largest in the various sulfuric acid solutions, while the concentration of Pb^{2+} ion has a maximum at 1 M H_2SO_4.

3. Cathodic reduction of $PbSO_4$ to Pb in sulfuric acid solution (charge reaction of the negative active material) [9]

The potentiodynamic current–voltage curves for the cathodic reduction of $PbSO_4$ to Pb in 1 M H_2SO_4 on the $Pb/PbSO_4$ electrode prepared from a Pb rod were determined, as shown in Fig. 5. The cathodic current rapidly increases and then gradually decreases. The peak currents increase with increasing sweep rate and change linearly with the square root of the sweet rate. Same change is obtained in the case of the semi-infinite linear diffusion controlled current on a planer electrode. However, in this case, the diffusion of the Pb^{2+} ion is not explained by semi-infinite linear diffusion, because the electrochemical reaction takes place where both $PbSO_4$ and Pb exist.

Thus, the reaction site model illustrated, as shown in Fig. 6(A) was proposed. In this model, it is assumed that the Pb^{2+} ions are transported from the $PbSO_4$ crystal surface to the Pb surface and then reduced on the Pb of electronic conductor. The reaction rate depends on the electrochemical kinetic parameters, e.g., exchange charge-transfer rate, the real area of the interface between the $PbSO_4$ and the Pb and the mass-transfer of Pb^{2+} ions. The gap between the $PbSO_4$ and the Pb may be narrow, and the diffusion phenomena in such a gap can be assumed to be like those in a thin layer cell, as in Fig. 6(B). The concentration profile of Pb^{2+} ions is illustrated in Fig. 6(C), and the $PbSO_4$

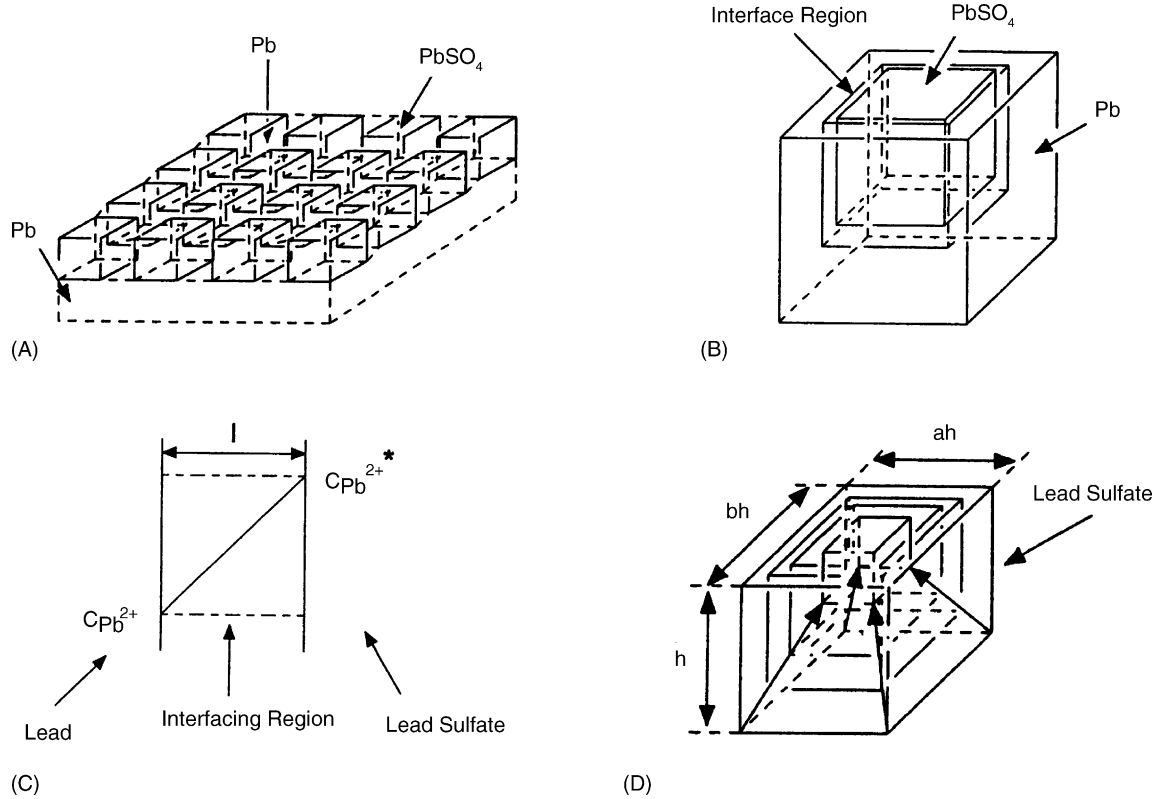

Fig. 6. The schematic illustrations of the $PbSO_4$ crystals deposited on the Pb surface (A), the model of the reaction site (B), the concentration profile of Pb^{2+} ions at the interface region (C), the change of the $PbSO_4$ crystal during the cathodic reduction (D).

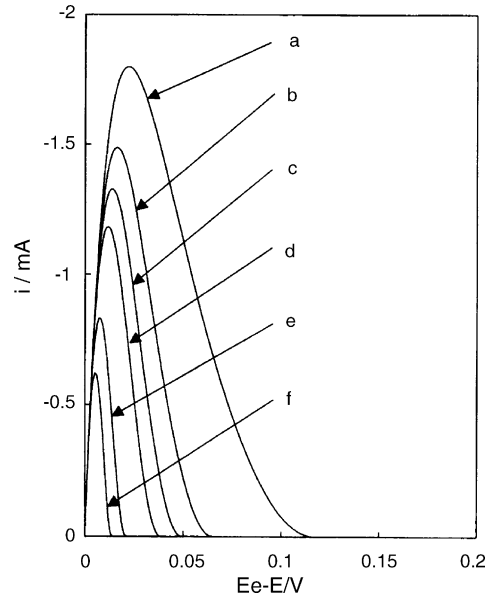

Fig. 7. Calculated current–potential curves for the cathodic reduction of $PbSO_4$ to Pb at various sweep rates: (a) 20 mV s^{-1}; (b) 10 mV s^{-1}; (c) 7 mV s^{-1}; (d) 5 mV s^{-1}; (e) 2 mV s^{-1}; (f) 1 mV s^{-1}.

crystal becomes smaller as in Fig. 6(D). By using this model, the current–voltage curve for a single $PbSO_4$ crystal is calculated. Then, the total current is calculated by the multiplication of the number $PbSO_4$ crystal.

Since the exchange current density is estimated to be the order of 1–10 mA cm^{-2}, the rate-determining step for the reduction of $PbSO_4$ to Pb is controlled by the mass-transfer. Then, the current–voltage curves were calculated at various sweep rates, under following conditions; the concentration of Pb^{2+} ions: 2.4×10^{-5} M, the diffusion coefficient: 5×10^{-6} cm^2 s^{-1}, the height of a single $PbSO_4$ crystal: 1 μm, its length: 1 μm, its width: 1 μm, the diffusion path length: 5×10^{-3} μm, and the volume of $PbSO_4$ crystal: 1.2×10^{-6} cm^3. The calculated curves are similar to those observed in Fig. 5, as shown in Fig. 7. However, the observed curves show some deviation from the calculated curves, due to the distribution of $PbSO_4$ crystal sizes and the uncertainty of estimating the number of $PbSO_4$ crystals.

From the above model, it can be expected that the large crystal size gives a smaller reaction site area per unit volume, and a large solubility of $PbSO_4$ gives a large current. The cathodic reduction of the negative active material strongly depends on the crystal size and the solubility of $PbSO_4$ crystals.

4. Oxidation of $PbSO_4$ at the interface between the grid and the active material [10–12]

The porous β-PbO_2 prepared from a paste active material (thickness of about 2 mm) on a Pb plate was discharged in 2.5 M H_2SO_4 at 8 mA cm^{-2}, and then potentiostatic discharged at −450 mV versus $PbO_2/PbSO_4$ at 30 °C. The electrode surface and the interface between the active material and a Pb plate were observed under the conditions before discharge, before and after potentiostatic discharge during 5 days by SEM, as shown in Fig. 8. No $PbSO_4$ crystals are observed on the surface before discharge. After discharge, surface is covered with the $PbSO_4$ crystals of size about 20–30 μm. Most of the $PbSO_4$ crystals on the electrode surface are formed during the galvanostatic discharge, while further crystals are formed within the inner part of the elec-

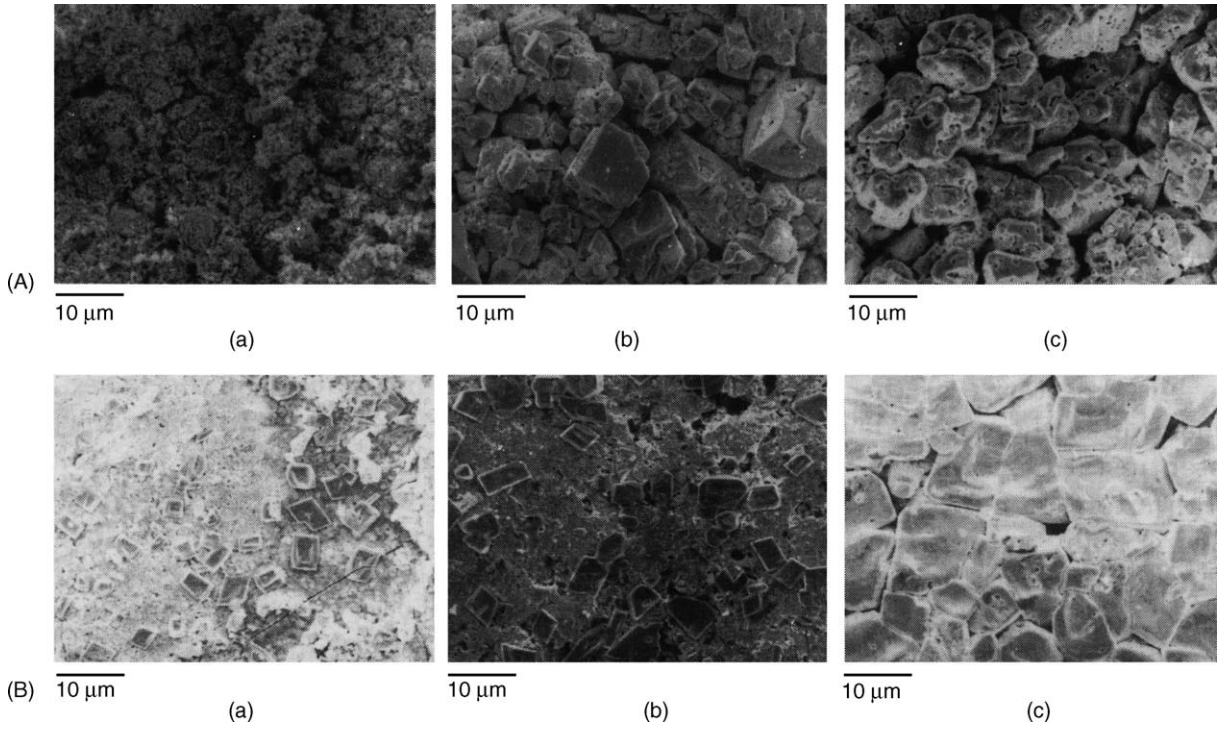

Fig. 8. The porous β-PbO_2 electrode surface (A), and the interface between a Pb plate and the porous electrode (B): (a) before discharge, (b) before potentiostatic discharge, (c) after potentiostatic discharge during 5 days, observed by SEM.

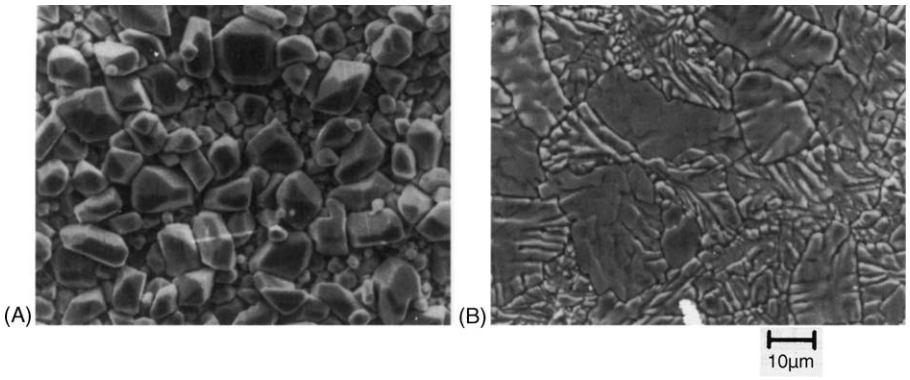

Fig. 9. The β-PbO_2 electrode surface (A), and the interface between a gold plate and the β-PbO_2 film (B), discharged for 2 days at 50 °C, observed by SEM.

trode during the following potentiostatic discharge. The $PbSO_4$ crystals do not grow at the interface during the galvanostatic discharge. Then, the $PbSO_4$ crystals develop at the interface during the potentiostatic discharge. And then, the whole of the interface is covered with the large and plate-like $PbSO_4$ crystals during the course of the following potentiostatic discharge of 5 days.

The growth rate in a parallel direction to the substrate at the interface region may be larger than that in a perpendicular direction, because it is limited by the substrate. The discharge reaction rate at the interface region is slow because of the slow mass transport. The crystal size of $PbSO_4$ increases with the decrease in the discharge current. Moreover, the concentration of sulfuric acid solution at the interface decreases with the extent of the discharge reaction because the sulfuric acid is consumed and the diffusion rate through the β-PbO_2 film is not sufficient. The solubility of $PbSO_4$ in sulfuric acid solution increases with decreasing the concentration from 5 to 1 M H_2SO_4. The recrystallization process rate increases with increasing solubility of $PbSO_4$. Thus, the large and plate-like $PbSO_4$ crystals will be formed at the interface between the active material and a Pb plate. Such an electrode was potentiostatic charged at +200 mV versus PbO_2/$PbSO_4$ in 2.5 M H_2SO_4 at 30 °C. The charge acceptance of an electrode discharged under galvanostatic condition is very good. However, in the case of electrode, galvanostatic and then potentiostatic discharged for 5 days, a constant very small current, which is caused by the resistance layer formed on the interface is observed.

In order to know clearly the characteristics of the plate-like $PbSO_4$ crystals, a dense β-PbO_2 film on a gold plate (thickness 30–40 μm) was discharged at 50 μA cm^{-2}, and then potentiostatic discharged at −420 mV versus PbO_2/$PbSO_4$ in 5 M H_2SO_4 for 2 days at 50 °C. The electrode surface and the interface between a gold plate and the β-PbO_2 film were observed by SEM, as shown in Fig. 9. The $PbSO_4$ crystals of large and plate-like exist at the interface between a gold plate and the β-PbO_2 film. The change of β-PbO_2 to $PbSO_4$ produces stress in the film due to the difference in the molar volumes of β-PbO_2 and $PbSO_4$. Thus, a dense β-PbO_2 film cracks during the course of potentiostatic discharge at 50 °C. Sulfuric acid solution penetrates through such cracks and, as the result, $PbSO_4$ crystals are formed at the interface between a gold plate and the β-PbO_2 film.

Though the lead–acid battery has higher equilibrium voltage of about 2.04 V than the equilibrium voltage of the water decomposition, 1.23 V, the water decomposition is controlled due to the high over-potential of oxygen evolution on the β-PbO_2 and that of hydrogen evolution on the Pb. But, it is impossible to avoid the self-discharge on the positive and the negative active materials. These come from the formation of a local cell consisting of either the anodic reaction of oxygen evolution on the β-PbO_2 or the cathodic reaction of hydrogen evolution on the Pb. The self-discharge with small current causes the formation of the large, plate-like $PbSO_4$ crystals on the interface between the active materials and the grid materials. Thus, the floating charge at the more positive potential than the equilibrium potential of β-PbO_2/$PbSO_4$ electrode and the more negative potential than the equilibrium potential of Pb/$PbSO_4$ electrode is necessary. The upper limit of the floating potential of the positive electrode must be restricted by the corrosion of the grid materials.

Acknowledgments

I would like to thank to Prof. emer. Shiro Yoshizawa (the deceased) for his valuable direction and suggestions, and also would like to thank to Prof. Zempachi Ogumi and Prof. Kiyoshi Kanamura for their helpful suggestions and discussions.

References

[1] Z. Takehara, J. Power Sources 30 (1990) 55–75.
[2] Z. Takehara, J. Power Sources 85 (2000) 29–37.
[3] Z. Takehara, K. Kanamura, Electrochim. Acta 29 (1984) 1643–1648.
[4] Z. Takehara, K. Kanamura, Bull. Chem. Soc. Jpn. 60 (1987) 1567–1572.
[5] Z. Takehara, K. Kanamura, M. Kawanami, J. Electrochem. Soc. Jpn. 57 (1989) 475–479.
[6] Z. Takehara, K. Kanamura, J. Electrochem. Soc. 134 (1987) 13–18.
[7] Z. Takehara, K. Kanamura, J. Electrochem. Soc. 134 (1987) 1604–1610.
[8] Z. Takehara, K. Kanamura, M. Kawanami, J. Electrochem. Soc. Jpn. 57 (1989) 734–739.
[9] K. Kanamura, Z. Takehara, J. Electrochem. Soc. 139 (1992) 345–351.
[10] Z. Takehara, K. Kanamura, M. Kawanami, J. Electrochem. Soc. 137 (1990) 800–804.
[11] Z. Takehara, K. Kanamura, M. Kawanami, J. Electrochem. Soc. 136 (1989) 620–625.
[12] S. Yoshizawea, Z. Takehara, T. Honda, J. Electrochem. Soc. Jpn. 36 (1968) 740–745.